2009 American Control Conference
Hyatt Regency Riverfront, St. Louis, MO, USA
June 10-12, 2009

Data-driven Estimation of Multiple Fault Parameters in Permanent Magnet Synchronous Motors★

Subhadeep Chakraborty† szc108@psu.edu
Chinmay Rao† crr164@psu.edu
Eric Keller† eek105@psu.edu
Asok Ray† axr2@psu.edu
Murat Yasar‡ yasarm@technosci.com

***Abstract*— This paper presents symbolic analysis of time series data for estimation of multiple faults in permanent magnet synchronous motors ($PMSM$). The analysis is based on an experimentally validated dynamic model, where the flux linkage of the permanent magnet and friction in the motor bearings are varied in the simulation model to represent different stages of degradation. The fault magnitudes are estimated from the time series of the instantaneous line current. The behavior patterns of the $PMSM$ are compactly generated as quasi-stationary state probability histograms associated with the finite state automata of its symbolic dynamic representation. The proposed fault estimation method is suitable for real-time execution on a limited-memory platforms, such as those used in sensor network nodes.**

***Index Terms*— Symbolic Dynamics; Parameter Estimation; Electric Motors.**

1. INTRODUCTION

The role of electrical and electronic systems is ever expanding in all aspects of modern life. Particularly, for extreme operating conditions, lightweight, reliable primary power sources, auxiliary systems and backup storage have turned out to be increasingly essential and critical components. Several innovations in the design of modern direct drive motor/generator, power conversion and storage technologies have been made in recent years. In addition, it is now possible to replace several of the traditional mechanical, hydraulic and pneumatic mechanisms with electrical configurations. As industrial applications become complex, their functional reliability becomes increasingly dependent on healthy operation of the electrical motor and the associated electronics, which makes power system prognostics, diagnostics and health management an imperative technology. The goal is to achieve increasingly reliable, safe and low-cost power systems by exploiting the recent advances in embedded sensing and digital information processing.

★ This work has been supported in part by NASA under Cooperative Agreement No. NNC04GA49G and Contract No. NNC07QA08P.

†Mechanical Engineering Department, The Pennsylvania State University, University Park, PA 16802

‡Systems Engineering Department, Techno-Sciences, Inc., Beltsville, MD 20705-3194

The present paper reports an advancement to these data processing techniques by estimating the health condition of a motor, which is gradually deteriorating due to the simultaneous presence of two different fault sources, from readings obtained via a single sensor. Often evolution of gradual deviations from the nominal behavior in systems is an effect of simultaneous deterioration of two or more components, each of which might be harmless in itself, but in conjunction, may lead to cascaded faults because of strong input-output and feedback interconnections between the system components, and may eventually cause catastrophic failures and forced shutdown of the entire system. In such a scenario, the problem of degradation monitoring of the system reduces to simultaneous estimation of several slowly-varying critical parameters.

The primary thrust of the proposed research is to develop techniques for reliable real-time monitoring of multiple incipient faults in power system components such as generators and electric motors. The proposed algorithm that involves both signal preprocessing and symbolic dynamic filtering has been applied to a simulation model of a surface mounted Permanent Magnet Synchronous Motor ($PMSM$). This facility is particularly relevant for testing condition monitoring algorithms, since $PMSM$ are being increasingly used in commercial and military applications. For example, both commercial and fighter aircraft use $PMSM$ as critical components. An early indication about their performance deterioration is important.

In this algorithm, statistical patterns of the evolving system dynamics are identified from these symbol sequences through construction of probabilistic finite-state automata (*PFSA*). The state probability vectors that are derived from the respective state transition probability matrices of *PFSA* serve as behavioral patterns of the evolving dynamical system under nominal and off-nominal conditions. A key feature of the reported work is statistical fusion of evidence to obtain a probabilistic estimate of simultaneously varying parameters.

The fundamentals of the symbolic time series analysis is explained in the next section. The simulation model of the

$PMSM$ has been developed in Section 3 with the analysis of failure modes and results following in Section 4. The paper is concluded with recommendations for future research in Section 5.

2. Review of Symbolic Dynamic Filtering and Multiple-parameter Estimation

This section succinctly reviews the theory of symbolic dynamic filtering (*SDF*) [10] and explains the underlying concept of multiple parameter estimation [8] in the SDF framework.

Extraction of statistical behavior patterns from time series data is posed as a two-scale problem. The *fast scale* is related to response time of the process dynamics. Over the span of data acquisition, dynamic behavior of the system is assumed to remain invariant, i.e., the process is quasi-stationary at the fast scale. In other words, variations in the system parameters are assumed to be negligible on the fast scale. The *slow scale* is related to the time span over which deviations (e.g., parametric changes) may occur and exhibit non-stationary dynamics.

A. Construction of Symbolic Dynamic Patterns

This subsection summarizes the construction of behavior patterns for detection of deviation from nominal behavior in the SDF setting.

1) *Time series data acquisition on the fast scale from sensors and/or analytical measurements (i.e., outputs of a physics-based or an empirical model)*. Data sets are collected at slow-scale epochs, hereafter called epochs.
2) *Generation of wavelet/Hilbert transform coefficients with an appropriate choice of the wavelet basis and scales*. The wavelet and Hilbert transforms largely alleviate the difficulties of phase-space partitioning and are particularly effective with noisy data from high-dimensional dynamical systems.
3) *Maximum Entropy Partitioning of the transformed space at a reference condition*. This partitioning scheme ensures that the regions rich in information are partitioned finer and those with sparse information are partitioned coarser. Maximum entropy is achieved by a partition that produces a uniform probability of all partitions (cells). Partition once obtained is kept fixed for further calculations. Each segment of the partitioning is assigned a particular symbol from the symbol alphabet Σ. This step enables transformation of time series data from the continuous domain to the symbolic domain [5].
4) *Construction of a probabilistic finite state automaton (PFSA) at the reference condition*. The structure of the finite state machine is fixed for subsequent epochs until a new reference is selected.
5) *Computation of the reference pattern vector* $\mathbf{p}^0$ *whose elements represent state occupation probabilities of the PFSA at the reference condition*. Such a pattern vector is recursively computed as an approximation of the natural invariant density of the dynamical system, which is a fixed point of the local Perron-Frobenius operator [1]. Thus, $\mathbf{p}^0 \equiv [p_1^0\ p_2^0\ \cdots\ p_n^0]$, where n is the number of states in the *PFSA*.
6) *Time series data acquisition on the fast scale at subsequent epochs,* $t_1, t_2, ...t_k...$*, and their conversion to respective symbolic sequences based on the reference partitioning at epoch* t_0.
7) *Generation of the pattern vectors,* $\mathbf{p}^1, \mathbf{p}^2, ..., \mathbf{p}^k...$ *at epochs,* $t_1, t_2, ...t_k...$ *from the respective symbolic sequences using the state machine constructed at epoch* t_0. Thus, $\mathbf{p}^k \equiv [p_1^k\ p_2^k\ \cdots\ p_n^k]$, where n is the number of states in the *PFSA*. Note that the structure of the *PFSA* at all epochs is identical while the pattern vectors $\mathbf{p}^k$ are possibly different at different epochs. k.
8) *Computation of deviation measures*: Evolving deviation measures $\mathcal{M}_1, \mathcal{M}_2, ..., \mathcal{M}_k, ...$ at epochs, $t_1, t_2, ..., t_k, ...$, are computed with respect to the nominal condition at t_0, by selecting an appropriate distance function $d(\bullet, \bullet)$ (e.g., the standard Euclidean norm) such that $\mathcal{M}_k \triangleq d(\mathbf{p}^k, \mathbf{p}^0)$.

B. Forward Problem/Training

For the forward problem, sets of time series data are generated for each $\underline{s} \in \mathcal{S}$ at epochs t_k, $k = 1, 2, \cdots, |\mathcal{S}|$, for which experimental runs are conducted to generate the contour plot. A symbolic dynamic filter is constructed to analyze each data sequence as outlined in Subsection 2-A. For n being the number of automaton states, the n-dimensional pattern vector $\mathbf{p}^k(\underline{s})$ is generated for every $\underline{s} \in \mathcal{S}$, where $k = 1, 2 \ldots, |\mathcal{S}|$. For a given $\underline{s}$, let $\mathbf{p}^k(\underline{s}) \triangleq [p_1^k\ p_2^k\ \cdots\ p_n^k]^T$, where the superscript k represents an epoch and the subscripts denotes the state number ranging from 1 to n. For each $j = 1, 2, \cdots, n$, a random variable $q_j(\underline{s})$ is constructed from the ensemble of $k = 1, 2, \cdots, |\mathcal{S}|$ data points to represent the uncertain occupation probability of the j^{th} state of the the automaton in the SDF setting.

$$\mathbf{q}(\underline{s}) \equiv \begin{bmatrix} q_1(\underline{s}) & q_2(\underline{s}) & \ldots & q_n(\underline{s}) \end{bmatrix} \tag{1}$$

where $q_j(\underline{s}) \sim \mathcal{N}\left[m_j(\underline{s}), \sigma_j^2(\underline{s})\right]$, i.e., $q_j(\underline{s})$ is assumed to be Gaussian with mean m_j and variance $\sigma_j^2(\underline{s})$ as explained

below from the perspectives of state machine construction in the SDF setting.

The Symbolic dynamic filter models the underlying dynamical system as an irreducible Markov process, where the state probability vector is the sum-normalized eigenvector of the state transition matrix corresponding to the unique unity eigenvalue. Hence, no element in the state probability vector is either 0 or equal to 1. However, due to process noise, sensor noise and small uncertainties in parameter vector $\underline{s}$, the random variable $q_j(\underline{s})$ fluctuates around its mean $m_j(\underline{s})$. While analyzing the experimental data, the standard deviation $\sigma_j(\underline{s})$ of the random variables $q_j(\underline{s})$ was found to be very small compared to its expected value $m_j(\underline{s})$, i.e., the ratio $\frac{\sigma_j(\underline{s})}{m_j(\underline{s})} \ll 1 \; \forall \underline{s} \in \mathcal{S} \; \forall j = 1, 2, \cdots, n$. Therefore, a parametric or non-parametric two-sided unimodal distribution should be adequate to model the random variable $q_j(\underline{s})$.

Remark 2.1: The random variables $q_j(\underline{s})$ must satisfy the following two conditions:

- Positivity, i.e., $q_j(\underline{s}) > 0 \quad \forall \underline{s} \in \mathcal{S} \quad \forall j = 1, 2, \cdots, n,$. This is made possible by truncating the far end of the Gaussian distribution tail on the left side. The goodness of fit of the distribution as Gaussian still remains valid at a very high significance level.
- Unity sum of the state probabilities, i.e., $\sum_{j=1}^{n} q_j(\underline{s}) = 1 \; \forall \underline{s} \in \mathcal{S}$. This is achieved by sum-normalization.

Remark 2.2: The automaton states are analogous to energy states in statistical mechanics of ideal gases [6]. This fact is used formulating the Inverse problem as explained below.

C. Inverse Problem/Testing

Time series data are generated for identification of multiple parameters $\underline{s} \in \mathcal{S}$. The data are analyzed using the same symbolic dynamic filter constructed in the forward/training problem (see Subsection 2-A), and the resulting random vector is obtained as: $\mathbf{q}^{\text{test}} \equiv \begin{bmatrix} q_1^{\text{test}} & q_2^{\text{test}} & \cdots & q_n^{\text{test}} \end{bmatrix}$. The likelihood function $P(\underline{s}|\mathbf{q}^{\text{test}})$ is given by

$$P(\underline{s}|\mathbf{q}) = \frac{P\left(\mathbf{q}^{\text{test}}|\underline{s}\right) P(\underline{s})}{P\left(\mathbf{q}^{\text{test}}\right)} \tag{2}$$

$$= \frac{P\left(\mathbf{q}^{\text{test}}|\underline{s}\right) P(\underline{s})}{\sum_{\tilde{\underline{s}} \in \mathcal{S}} P\left(\mathbf{q}^{\text{test}}|\tilde{\underline{s}}\right) P(\tilde{\underline{s}})} \tag{3}$$

In the absence of a priori information, an assumption is made that all operating conditions are equally likely, i.e.,

$$P(\underline{s}) = \frac{1}{|\mathcal{S}|} \quad \forall \underline{s} \in \mathcal{S} \tag{4}$$

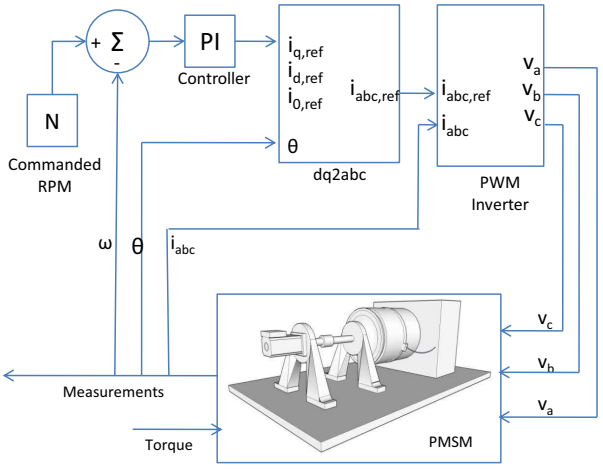

Fig. 1. Inverter-driven permanent magnet synchronous motor (*PMSM*) system

The above assumption of unbiased probability leads to:

$$P(\underline{s}|\mathbf{q}^{\text{test}}) = \frac{P\left(\mathbf{q}^{\text{test}}|\underline{s}\right)}{\sum_{\tilde{\underline{s}} \in \mathcal{S}} P\left(\mathbf{q}^{\text{test}}|\tilde{\underline{s}}\right)} \tag{5}$$

It is noted that accuracy of the above distribution would be improved if the actual probabilistic risk mapping is known.

As stated in the previous section, each random variable q_j that is related to occupation probability of the state j could be modeled by a parametric or non-parametric two-sided unimodal distribution. Therefore, the choice of Gaussian distribution for q_j would facilitate estimation of the statistical parameters and involve only second order statistics. This assumption has been validated by using the χ^2 and Kolmogorov-Smirnov tests for goodness of fit [2] of each q_j for Gaussian distribution. In this context, each random variable q_j is postulated to be Gaussian with a mean value m_j and variance σ_j^2.

The parameters of the conditional probability distribution $P\left(q_j^{\text{test}}|\underline{s}\right)$ are evaluated from the mean and variance of the state occupation probability at $\underline{s}$ and the resulting Gaussian distribution is obtained as

$$P\left(q_j^{\text{test}}|\underline{s}\right) = \frac{1}{\sqrt{2\pi\sigma_j^2(\underline{s})}} \quad \exp\left(\frac{-(q_j^{\text{test}} - m_j(\underline{s}))^2}{2\sigma_j^2(\underline{s})}\right) \tag{6}$$

Furthermore, it has been observed from experimental data that fluctuations of q_j are uncorrelated with those of q_k for all $j \neq k$. Therefore, the jointly Gaussian distribution of all q_j's can be reduced to the product of individual Gaussian distributions of the random variables.

The assumption of statistical independence of fluctuations of the $(n-1)$ elements of the random vector $\mathbf{q}^{\text{test}}$ for a given

parameter pair $\underline{s}$ permits the joint probability distribution in Eq. (5) to be converted into a product of individual distributions.

$$P(\underline{s}|\mathbf{q}^{\text{test}}) = \frac{\prod_{j=1,2,\ldots,n-1} P\left(q_j^{\text{test}}|\underline{s}\right)}{\sum_{\underline{\tilde{s}}\in\mathcal{S}} \prod_{j=1,2,\ldots n-1} P\left(q_j^{\text{test}}|\underline{\tilde{s}}\right)} \tag{7}$$

A most likely estimate of $\underline{s}$ is obtained from the probabilistic map in Eq. (7).

3. Description of the Simulation Experiment

This section describes the simulation model that is a representation of an inverter-driven permanent magnet synchronous motor (*PMSM*) [7], as depicted in Fig. 1. The simulation model of a generic $PMSM$, without a damper winding, is similar to that of a wound-rotor synchronous machine under the following simplifying assumptions:

- Negligible magnetic field saturation;
- Negligible eddy current loss and hysteresis loss;
- Negligible field current dynamics;
- Sinusoidal induced electromotive force (EMF);

In rotor reference frame, the governing equations of the stator voltage are given as:

$$v_q = Ri_q + \frac{d\lambda_q}{dt} + \omega_s\lambda_d \tag{8}$$

$$v_d = Ri_d + \frac{d\lambda_d}{dt} - \omega_s\lambda_q \tag{9}$$

where the subscripts q and d have their usual significance of quadrature and direct axes in the equivalent 2-phase representation; and

$$\lambda_q = L_q i_q \qquad \text{and} \qquad \lambda_d = L_d i_d + \lambda_{af} \tag{10}$$

with v, i, and L being the corresponding axis voltages, stator currents and inductances; R and ω_s are the stator resistance and inverter frequency, respectively, while λ_{af} is the flux linkage of the rotor magnets with the stator.

The generated electromagnetic torque is expressed as:

$$T_e = 1.5P\left[\lambda_{af} i_q + (L_d - L_q) i_d i_q\right] \tag{11}$$

and the equation of motor dynamics is given by:

$$T_e = T_L + B\omega_r + J\frac{d\omega_r}{dt} \tag{12}$$

where P is the number of pole pairs, T_L is the load torque, B is the damping coefficient, ω_r is the rotor speed, and J is the moment of inertia. The rotor speed $\omega_r = \omega_s/P$.

In state-space setting, the governing equations of the $PMSM$ take the following form:

$$\frac{di_q}{dt} = \left(v_q - Ri_q - \omega_s L_d i_d - \omega_s\lambda_{af}\right)/L_q \tag{13}$$

$$\frac{di_d}{dt} = \left(v_d - Ri_d + \omega_s L_q i_q\right)/L_d \tag{14}$$

$$\frac{d\omega_r}{dt} = \left(T_e - T_L - B\omega_r\right)/J \tag{15}$$

In the control scheme shown in Fig. 1, i_d is forced to be zero. Consequently,

$$\lambda_d = \lambda_{af} \quad \text{and} \quad T_e = 1.5P\lambda_{af} i_q \tag{16}$$

In the above equation, the torque T_e is proportional to the quadrature axis current because the magnetic flux linkage λ_{af} is constant.

In the simulation test bed, the motor model is a three-phase four-pole device rated at $1.1\ kW$, $220\ V$, $3000\ rpm$ and is fed by a pulse-width-modulated (*PWM*) inverter. The stator resistance of the motor is $R_s = 0.05\ \Omega$; the quadrature-axis and direct-axis inductances are: $L_q = L_d = 6.35 \times 10^{-4} H$; the nominal flux linkage $\lambda_{af} = 0.192\ Wb$; the rotor inertia $J = 0.011\, kg\ m^2$; and the friction factor is $B = 0.001889\ kgm^2\ s$.

A simple hysteresis current controller has been employed for controlling the power circuit that drives the $PMSM$, as seen in Fig. 1. Two control loops have been employed. The inner loop regulates the motor's stator currents, while the outer loop uses a proportional-integral controller to regulate the motor's speed. In this control scheme, the line currents i_a, i_b and i_c are measured. The reference values are compared with the actual values of the currents, and the error signal, thus constructed is used for generating the gate turn on/off commands. In the present scenario a hysteresis band of $0.25A$ on either side of the reference current i is employed.

4. Failure Modes and Results

Failure due to demagnetization of the permanent magnet in both surface-mounted and buried-magnet $PMSM$s have been widely studied in literature [12]. Demagnetization can occur due to several reasons, notable among which are demagnetization due to a strong opposing magnetic field, and also due to high temperature.

A strong opposing magnetic flux can be created in the event of a short circuit between one terminal of the machine and the (normally) isolated neutral point of the machine, short circuit between two or three terminals of the machine and short circuit in one of the diodes or electronic valves of the inverter, giving rise to a direct current (DC) in the machine even in short circuit steady state.

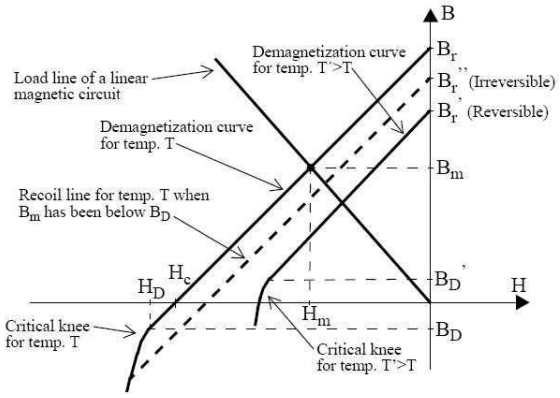

Fig. 2. Demagnetization property of Neodymium-Iron-Boron (Nd-Fe-B) [12]

Risk of irreversible demagnetization is present if the counter-acting flux lowers the flux density in the magnet to a point (H_D, B_D) that is just above the so-called critical knee of the magnets BH-curve, which has been illustrated in Fig. 2. The common method to check the demagnetization of the permanent magnets due to armature reaction is described in [4]. The disadvantage of this method is the assumption that the permanent magnet pole has uniform saturation. A more accurate way to check the demagnetization is with the finite element method.

Partial or complete demagnetization can also result from high temperature of the magnets and the winding insulation. The temperature increases the resistance of the winding wires and the increased resistance affects the applied current to the motor. At higher temperatures ($\sim 100^0C$), an appreciable deterioration in acceleration might be noticed, as the torque generated by a reduced magnetic flux drops below its nominal value.

Fatigue failure of bearings is quite common even under normal operating conditions with balanced load. Factors which affect smooth operation of the bearing are normal internal operating stresses caused by vibration, inherent eccentricity, and bearing currents due to solid state drives [3], as well as external causes, such as abnormal mounting. Ball bearing related defects manifest themselves as outer bearing race defect, inner bearing race defect, ball defect, and train defect. Specific information concerning the bearing construction is indispensable for predicting the exact failure characteristics. However it may be safely assumed, that all such performance deteriorations principally manifest themselves as increase in the bearing friction.

A. Results on simulation model

In this paper, health-monitoring of permanent magnet synchronous motors has been proposed by a nonlinear time series analysis technique called symbolic dynamic filtering in conjunction with Hilbert Transform Space Partitioning [11]. The motor described in Section 3 is simulated to undergo a steady deterioration in terms of permanent magnet flux linkage, due to either of the two reasons mentioned above. This is guaranteed by decreasing the flux linkage λ_{af} from its nominal value of $0.192Wb$ to $0.007Wb$ in incremental steps. At the same time the friction in the bearing is increased from the nominal value of $B = 0.5Nms$ to a value of $B = 1Nms$. The line current signals i_a, i_b, i_c, which in principle reflect both these deteriorations are collected from the motor output at each of these off-nominal partially-demagnetized state of the rotor running on bearings with gradually increasing friction.

This data is then Hilbert Transformed and converted into discrete symbols. Maximum Entropy partitioning is employed in the radial direction while the data is uniformly partitioned in the angular direction. The discretization procedure has been briefly discussed in Section 2 while details are available in previous publications [10] [9]. Here an alphabet size of $|\Sigma| = 15$ and a depth of $D = 1$ has been employed. This information on time series data was then fed into the *SDF* to compute the components p_j of pattern vectors **p** at different values of the parameter pair λ_{af}, B. The pattern vector obtained by constructing the D-Markov machine representation of the motor characterizes the health condition of the motor in general. As the dynamics of the PMSM system changed due to deterioration in flux linkage, as well as friction coefficient, the statistics of the symbol sequences were altered and so were the pattern vectors.

For the inverse problem, experiments were conducted at several random predetermined values of the parameters that were different from those in the forward problem/training of *SDF*. The components p_j of pattern vectors **p** at different values of the parameter pair were computed from the data sets that were generated with these assigned values of parameters. The parameter pair is crisply identified by a single, sharp spike in the probability distribution plot. Table I shows the results for mean and confidence intervals of the parameter estimates for four different test runs that did not belong to the set of training data. It is seen that the estimated mean values of the flux linkage (λ_{af}) and friction coefficient (B) are very close to their true values and are orders of magnitude greater than the respective standard deviations $\hat{\sigma}_{\lambda_{af}}$ and $\hat{\sigma}_B$.

TABLE I
PREDICTED VALUES OF $\left(\hat{\lambda}_{af}, \hat{B}\right)$ AND CONFIDENCE INTERVALS FOR THE $PMSM$

Test No.	Estimates									
	Parameter λ_{af}			Parameter B			95 % Confidence Interval		90 % Confidence Interval	
	$\lambda_{af}^{\text{test}}$	$\hat{\lambda}_{af}$	$\hat{\sigma}_{\lambda_{af}}$	B^{test}	$\hat{B}$	$\hat{\sigma}_B$	$(\lambda_{af_{\min}}, \lambda_{af_{\max}})$	$(B_{\min}, B_{\max})$	$(\lambda_{af_{\min}}, \lambda_{af_{\max}})$	$(B_{\min}, B_{\max})$
1	0.075	0.075	$1.6e-7$	0.60	0.60	$1.6e-8$	$(0.075, 0.075)$	$(0.60, 0.60)$	$(0.075, 0.075)$	$(0.60, 0.60)$
2	0.09	0.09	$6.2e-7$	0.80	0.80	1.2e-8	$(0.09, 0.09)$	$(0.80, 0.80)$	$(0.09, 0.09)$	$(0.80, 0.80)$
3	0.11	0.11	$1.5e-9$	0.70	0.70	$2.3e-8$	$(0.11, 0.11)$	$(0.70, 0.70)$	$(0.11, 0.11)$	$(0.70, 0.70)$
4	0.10	0.10	$3.8e-9$	0.90	0.90	$7.0e-9$	$(0.10, 0.10)$	$(0.90, 0.90)$	$(0.10, 0.10)$	$(0.90, 0.90)$

5. SUMMARY, CONCLUSIONS, AND FUTURE WORK

This paper addresses the issues of degradation monitoring in a simulated permanent magnet synchronous motor. The Degradation Monitoring algorithm is based on analysis of time series data observed from the motor. A simulated model of the $PMSM$ has been monitored for accelerated failure from two sources, namely degradation of the flux linkage of the permanent magnets and a slow increase in the bearing friction coefficient. The health condition estimated from analysis of the current signal has been found to be consistent with the actual degradation condition.

A. Pertinent Conclusions and Recommendations for future research

The above discussion evinces that SDF is potentially a useful tool for detecting various levels of multiple degradation combinations in the performance of electric motors. However, further theoretical, computational, and experimental research is necessary before the SDF-based anomaly detection tool can be considered for incorporation into the Instrumentation and Control system of commercial-scale plants using these motors.

- For example, an important issue, not addressed in this paper, is quality assurance and automated calibration [18] of the sensor time series data, because a sensor providing faulty signal at a particular time epoch, may lead to an incorrect estimate of the damage measure of interest.
- The inverse problem to the one discussed here is potentially beneficial in practical scenarios. The inverse problem involves prediction of the remaining life of the machine by inspecting the health condition estimated at a certain point of time in the slow time scale, and mapping that information to an already established bank of health condition data to estimate the available remaining useful service life of the motor under consideration. This might have a desirable impact on extending the service life of motors and prevent unscheduled shutdowns.

REFERENCES

[1] R.B. Bapat and T.E.S. Raghavan, *Nonnegative matrices and applications*, Cambridge University Press, Cambridge UK, Cambridge, U.K, 1997.

[2] H.D. Brunk, *An introduction to mathematical statistics,3rd edn.*, Xerox Publishing,Lexington, MA., 1995.

[3] S. Chen and T. A. Lipo, *Bearing currents and shaft voltages of an induction motor under hard- and soft-switching inverter excitation*, IEEE Trans. Ind. Appl **34** (Sep./Oct. 1998), no. 5, 1042–1048.

[4] J.R. Hendershot and T.J.E. Miller, *Design of brushless permanent-magnet motors*, Oxford University Press, 1996.

[5] D. Lind and M. Marcus, *An introduction to symbolic dynamics and coding*, Cambridge University Press, 1995.

[6] R.K. Pathria, *Statistical mechanics*, Elsevier Science and Technology Books, 1996.

[7] P. Pillay and R. Krishnan, *Modeling, simulation, and analysis of permanent-magnet motor drives, Part I: The permanent-magnet synchronous motor drive*, IEEE Transactions on Industry Applications **25** (1989), no. 2, 265–273.

[8] V. Rajagopalan, S. Chakraborty, and A. Ray, *Estimation of slowly varying parameters in nonlinear systems via symbolic dynamic filtering*, Signal Processing **88** (2008), no. 2, 339–348.

[9] C. Rao, A. Ray, S. Sarkar, and M. Yasar, *Review and comparative evaluation of symbolic dynamic filtering for detection of anomaly patterns*, Signal, Image and Video Processing (2008), DOI 10.1007/s11760-008-0061-8.

[10] A. Ray, *Symbolic dynamic analysis of complex systems for anomaly detection*, Signal Processing **84** (2004), no. 7, 1115–1130.

[11] A. Subbu and A. Ray, *Space partitioning via hilbert transform for symbolic time series analysis*, Applied Physics Letters **92** (2008), no. 8, 084107.

[12] P. Thelin, *Short circuit fault conditions of a buried pmsm investigated with FEM*, NORPIE/2002, Stockholm, Sweden, 2002.